British Journal of Pharmaceutical Research
6(4): 228-254, 2015, Article no.BJPR.2015.065
ISSN: 2231-2919

SCIENCEDOMAIN *international*
www.sciencedomain.org

Biocompatible and Biodegradable Chitosan / Clay Nanocomposites as New Carriers for Theophylline Controlled Release

Catalina Natalia Cheaburu-Yilmaz[1], Raluca Petronela Dumitriu[1], Manuela-Tatiana Nistor[1], Catalina Lupusoru[2], Marcel Ionel Popa[3], Lenuta Profire[2], Clara Silvestre[4] and Cornelia Vasile[1*]

[1]"P. Poni" Institute of Macromolecular Chemistry, 700487, Iasi, Romania.
[2]"Gr. T. Popa" University of Medicine and Pharmacy, 700115, Iasi, Romania.
[3]"Gh. Asachi" Technical University, 700050, Iasi, Romania.
[4]Institute of Chemistry and Technology of Polymers (ICTP), The National Research Council (CNR), Pozzuoli (NA), Italy.

Authors' contributions

This work was carried out in collaboration between all authors. Authors CNCY and CV designed the study, wrote the protocol, and wrote the first draft of the manuscript. Authors CNCY and RPD managed the literature searches. Authors RPD, MTN, CL, MIP and LP managed some of analyses of the study, statistics and toxicity and biocompatibility test protocols. Author CS managed thermal properties analyses and microscopic observations. All authors read and approved the final manuscript.

Article Information

DOI: 10.9734/BJPR/2015/16525
Editor(s):
(1) Sami Nazzal, College of Pharmacy, University of Louisiana at Monroe, USA.
Reviewers:
(1) Anonymous, Thailand.
(2) Anonymous, Turkey.
(3) Anonymous, Portugal.
Complete Peer review History: http://www.sciencedomain.org/review-history.php?iid=985&id=14&aid=8396

Original Research Article

Received 5th February 2015
Accepted 26th February 2015
Published 11th March 2015

ABSTRACT

Aims: Carrier polymeric materials based on chitosan and chitosan / montmorillonite crosslinked with glutaraldehyde were prepared and studied for their biocompatibility, nontoxicity, and biodegradability aiming their application in drug delivery.
Study Design: Polymeric materials based on chitosan and chitosan/ montmorillonite crosslinked with glutaraldehyde were prepared as new carriers for theophylline release.
Methodology: The matrices of chitosan / glutaraldehyde and chitosan / montmorillonite /

**Corresponding author: Email: cvasile@icmpp.ro, duncaty@gmail.com;*

glutaraldehyde were prepared, purified and lyophilized to obtain porous materials. The biocompatibility and toxicity of the samples were tested by means of specific tests determining the life rate of white Swiss mice after intraperitoneal injection of the polymeric matrices prepared as suspensions; hemocompatibility was evaluated by hemolysis test with human blood and cell viability tests were performed by chemiluminescence assay. The matrices loaded and unloaded with theophylline were characterized in terms of structural changes, thermal stability, chemical and enzymatic degradation, distribution of the active substance, etc. In order to demonstrate the drug carrier ability of these matrices, theophylline release studies were performed both by *in vitro* and *in vivo tests*.

Results: The *in vivo* release profiles showed the sustained release of theophylline proved by the drug presence recorded up to 50 h from administration time.

Conclusion: An improvement of the half-release time ($t_{1/2}$) from 12 to 14 hours was obtained in vivo in the case of the matrix containing montmorillonite, indicating the possibility of reduced dosing frequency, but with a prolonged action time, which is beneficial to the patient.

Keywords: Chitosan; montmorillonite; biocompatibility; biodegradability; theophylline; retarded drug release.

1. INTRODUCTION

A targeted drug delivery system is composed of three components: a therapeutic agent, a targeting moiety and a carrier system. The drug can be either incorporated by passive absorption or by chemical conjugation into the carrier system. The choice of the carrier molecule is of high importance because it significantly affects the pharmacokinetics and pharmacodynamics of the drugs. Since the advent of timed-release pharmaceuticals, scientists have faced with the problem of finding new ways to deliver drugs to a particular site in the body without being first degraded in the highly acidic environment of the stomach.

In last years, much attention has been paid to the development of hydrogels from natural sources, natural polymeric materials being biodegradable, biocompatible and non-toxic for human body. Among the drug carriers, polysaccharides have received increasing attention because of their outstanding physical and biological properties. Within the past 20 years, a considerable amount of work has been published on chitosan, a linear polysaccharide comprising β-1,4 linked glucosamine and N-acetyl-D-glucosamine moieties, and its potential use in drug delivery systems was intensively reported [1-3]. Chitosan has a cationic character because of its primary amine groups and possesses great crosslinking ability. These primary amine groups are responsible for properties such as pH sensibility, controlled drug release, mucoadhesion, *in situ* gelation, transfection and permeation enhancement. The main drawback of chitosan is the low solubility in organic solvents and therefore the chemical modifications are needed for improvement of its properties, including solubility in various organic solvents.

An alternative for developing higher performance materials regarding the drug release abilities is using montmorillonites to obtain hybrid materials. Clay minerals play a crucial role in modulating drug delivery due to their large specific surface area, good adsorption ability, cation exchange capacity, standout adhesive ability, and drug-carrying capability. Therefore, hybrid materials based on nanocomposites of clay minerals and biopolymers for pharmaceutical applications can combine the properties of both components (inorganic and organic), such as swelling/water uptake mechanical characteristics, thermal behavior, rheology and bio-adhesion. Among them, montmorillonite / chitosan nanocomposites are receiving great attention, especially for biomedical (tissue engineering) [4-6] and pharmaceutical (retarded release) applications [7-9]. Chitosan chains have been described to intercalate with Na^+MMT, because of their hydrophilic and cationic character, giving to the new hybrid nanocomposite material with interesting swelling properties, improved mechanical and thermal characteristics and bio-adhesion [10]. Other reports confirm that the concentration of the inorganic silicate layers within the chitosan matrix is a critical parameter to achieve materials with enhanced properties (mechanical, thermal and/or electro-stimuli response) compared with the pure components [11-14].

With this respect, Liu et al. [15] showed that nanocomposite hydrogels containing 2 wt%

montmorillonite showed improved release behavior of vitamin B12, compared with the pure chitosan. Yuan et al. [16] reported that the ratio between montmorillonite and chitosan was a key factor also in the case of nanocomposites prepared to control the release of chemotherapeutic agent doxorubicin. pH-dependent release profiles were found for these nanocomposites, which were described as promising supports for colonic prolonged drug delivery. The majority of the studies are devoted to the physical-chemical and pharmaceutical characterization of montmorillonite / chitosan nanocomposites. Also their biocompatibility for drug release has been evaluated [17-19]

In our previous work, a nanocomposite based on chitosan and montmorillonite was prepared by simple solid–liquid interaction and the effective polymer/clay intercalation was confirmed by thermal analysis, mechanical properties, XRD patterns and microscopy [11]. It was reported that up to 5 wt% clay content the nanocomposites containing different clay types showed enhanced mechanical and thermal properties as well as improved swelling and drug delivery abilities [20]. It was also shown that the clay concentration plays a crucial role in drug release characteristics of the biomaterials [21].

The present study aims a detailed report on the biodegradability, biocompatibility and non-toxic character of the matrices based on chitosan (CS) / sodium montmorillonite (Na^+MMT) crosslinked with glutaraldehyde (GA) by means of different biocompatibility and toxicity assays and biodegradation studies. The active substance used was theophylline (1,3-dimethylxanthine) (THP) which is an alkaloid found in the leaves of *Camellia sinensis* and is used clinically as a bronchodilator in the management of chronic obstructive pulmonary diseases. THP has a short half-life (6 h), therefore, the conventional dosage forms must be administered 3-4 times a day in order to avoid large fluctuations in plasma concentration. The therapeutic effects of THP appear for plasma concentration between 5 and 10 µg/mL and toxic effects occur frequently for concentrations above 20 µg/mL [22]. Due to its numerous side-effects, this drug is now rarely administered as it is. Sustained release dosage forms for THP provide desirable serum concentrations for prolonged periods without frequent dosing, thereby preventing the complications in the therapy of patients [23]. THP is soluble both in acidic and alkaline medium.

The outcomes of our studies were the retarded *in vitro* and *in vivo* release of theophylline from CS/GA and CS/Na^+MMT/GA hydrogels proving their efficiency as drug delivery vehicles in pharmaceutical formulations.

2. MATERIALS AND METHODS

2.1 Materials

Chitosan used in the study was an Aldrich product, with an average molecular weight of 400 kDa and a deacetylation degree of about 68% determined by Moore and Roberts's method on the base of FT-IR spectrum. Glutaraldehyde used as crosslinking agent was purchased from Fluka as a 50 wt% solution. Sodium Montmorillonite (Na^+MMT) is a natural unmodified montmorillonite from Southern Clay Product Inc - Rockwood Additives Ltd. Anhydrous theophylline (THP) was purchased from Sigma–Aldrich. All the other materials and reagents used in this study were of analytical grade. Two series of samples have been investigated namely: I. Chitosan crosslinked with glutaraldehyde abbreviated with CS/GA and, II. Chitosan / sodium montmorillonite crosslinked with GA (CS/Na^+MMT/GA).

2.1.1 Preparation of the chitosan-based hydrogel

Chitosan (CS) solutions (1 g/dL) were prepared in 1 g/dL acetic acid solution by continuous stirring for about 4 hours until complete dissolution of chitosan. The sample of chitosan was cross-linked with glutaraldehyde (GA) with a molar ratio CS: GA of 1:0.33 obtaining a yellowish transparent gel.

2.1.2 Preparation of the hybrid hydrogel nanocomposite

The chitosan / montmorillonite nanocomposites were obtained via the solution mixing technique. Prior to mixing with the clay, the chitosan solution with a concentration of 1 g/dL was prepared in 1 g/dL acetic acid solution. Separately the clay dispersion in a small amount of acetic acid solution (1 g/dL) was prepared, sonicated for 10 minutes and then left overnight. The clay dispersion was added to the chitosan solution in small amounts under continuous stirring for about 4 hours. The amount of clay within the chitosan solution was 5 wt % (based on chitosan weight). Furthermore the newly prepared solution based on chitosan and nanoparticles was treated

with a diluted solution of glutaraldehyde using a molar ratio of 1: 0.33 for chitosan/Na^+MMT: GA.

The prepared chitosan cross-linked with GA and chitosan/ Na^+MMT crosslinked with GA hydrogels were intensively purified by dialysis (molecular weight cut-off 14,000 Da) against twice distilled water for 7 days at room temperature, until the measured pH in the washing water was 7, before to be tested for their toxicity and biocompatibility. Afterwards the gel-like samples were lyophilized using a freeze-drying system (LABCONCO Free- Zone) before investigation. The samples look like yellowish sponges, resistant to mechanical deformations.

2.2 Methods

2.2.1 Characterization of polymer matrices based on chitosan

The structure and relationship between the chemical structure and properties of the two polymer matrices based on chitosan were evidenced by using FT-IR spectroscopy, chemical and enzymatic degradation, swelling studies and biocompatibility and toxicity assays. The freeze-dried hydrogels based on chitosan with crosslinking agent with and without nanoparticles were spectroscopically analyzed, to evidence the structure differences between hydrogels of chitosan cross-linked with GA and the influence of clay on the matrix. The *ATR-FTIR spectra* were recorded using a Vertex 70 Bruker Spectrometer, through reflexion on a diamond crystal with an angle of 45 degrees.

Swelling capacity of the two matrices was investigated by direct immersion in acidic solution of pH 2.2 at 37°C, which simulates the gastric fluid medium conditions as *in vivo* experiments were done by oral administration. The hydrogel samples were periodically removed from the solution, gently wiped with a soft tissue to remove surface solution, weighed and then carefully placed back into the vessel as quickly as possible.

The swelling degree (S) was calculated according to the equation (1):

$$S(\%) = \frac{(W_t - W_d)}{W_d} \times 100 \quad (1)$$

Where: W_t is the weight of the swollen samples at time t and W_d is the weight of the dry sample.

To determine the kinetics of solvent diffusion into the matrices (swelling) the following equation was used [24]:

$$\frac{W_t}{W_{eq}} = k_{sw} * t^{n_{sw}} \quad (2)$$

Where: W_t and W_{eq} represent the amount of solution absorbed by the matrices at time t and at equilibrium, respectively; k_{sw} is the swelling rate constant or specific rate characteristic of the system and n_{sw} is the power diffusion law exponent which takes into account the type of solvent transport. Eq. (2) applies to initial stages of swelling (swelling degree less than 60%) where linearity of $ln\ F_t$ as a function of lnt is obtained.

The thermal behavior of the chitosan matrices loaded with theophylline was evaluated using a Q 500 (TA Instruments) thermal analyzer. The thermogravimetry (TG) was performed on samples of ~ 5 mg weight, in air flow, from 15 to 700ºC, at a heating rate of 20ºC min^{-1}.

The *in vitro* degradation was performed by treating the chitosan based materials, with and without nanoparticles, with buffered phosphate at a pH 5.5 with 10 mL chitosanase solution having the activity of 4.78 U/100 mL. The treated samples were kept further in oven under constant conditions at 37ºC. At different time intervals 1 mL from each type of sample was prelevated which content of N-acetyl D-glucosamine was analyzed by means of photocolorimetric method with potassium ferricianide. The degree of degradation and the concentration of N-acetyl D- glucosamine were determined. The degradation of chitosan based hydrogels in time was tested by immersing the samples in acidic medium with various pHs between 2.2 – 5.5. The samples were periodically removed from the solution, gently wiped with a soft tissue to remove surface solution and weighted.

The chemiluminescence assay was used for testing the capacity of chitosan based materials (i.e. CS/GA and CS/Na^+MMT/GA) of maintaining cells of *Schizosaccharomyces pombe*. The experimental assay was a similar one used by Yamashoji [25] and presented in detail in our previous study [26] as being highly sensitive and specific assay method for the detection of viable *Schizosaccharomyces pombe* wild type as an indicator organism in water, using Nucleic-Acid-

Sequence-Based. As result of the test, the cell viability in the presence of CS/GA and CS/Na^+MMT/GA was determined.

The hemocompatibility abilities of the samples based on chitosan i.e. CS/GA and CS/Na^+MMT/GA was done by means of hemolysis tests with human blood. The description of the method was previously explained [26]. The hemoglobin concentration from plasma was determined via the polychromatic method of Noe [27] the absorbance being measured at 380, 415 and 470 nm. As a result of this test, hemolysis degree was calculated.

Biocompatibility of the hydrogels of CS/Na^+MMT/GA was tested by means of toxicity tests and specific biocompatibility tests determining the life rate of white Swiss mice after intraperitoneal injection of solution of polymeric matrices. The specific parameters like the hemogram, the phagocytic capacity of neutrophils (NBT test), the opsonic capacity of serum, the phagocytic and bactericidal capacities of peritoneal macrophages and the hepatotoxic effects (through the enzymatic levels of aspartate aminotransferase (AST), serum alanine aminotransferase (ALT) and lactate dehydrogenase (LD)) were determined. Details over the methodology and protocols used for performing these tests were reported in a previous study on other polymeric matrices tested as carriers for sustained theophylline release [28].

2.2.2 Characterization of drug loaded matrices

The studied polymeric matrices namely CS/GA and CS/Na^+MMT/GA hydrogels loaded with theophylline as active substance were characterized by methods which emphasize the drug loading ability (adsorption and spectroscopic methods) as well as the morphology of the loaded hydrogels which prove the interactions of the drug with the polymeric matrices.

For *in vitro* release study CS/GA and CS/Na^+MMT/GA hydrogel samples loaded with theophylline were obtained by mixing the drug with the dried matrices in powder form (5 wt % drug reported to dry hydrogel) followed by swelling at room temperature for 1 h in a certain quantity of solvent for each composition studied which corresponds to the maximum quantity of liquid uptake measured during swelling experiments—while the drug penetrates and/or attached into the matrices. The solvent used was acidic solution of pH 2.2, the same conditions applied for the release study, too. The prepared physically bonded conjugates of theophylline-loaded samples were freeze-dried using a Lab Conco Free Zone device.

Prior to the *in vivo* experiments, the drug loaded polymeric matrices were prepared by diffusion filling method. In this way it was allowed the equilibrium partitioning of drug into the hydrogel [29] from a solution of 4 wt % drug concentration in ethanol/water 1/1 mixture which swells the polymer network. The drug-loaded hydrogels were prepared as suspensions, by swelling of 0.1 g of CS/GA and CS/Na^+MMT/GA hydrogels in powder form in the 4 wt % theophylline solution (1:1, v/v %, ethyl alcohol/ water) under mild stirring for 24 h period corresponding to the time necessary to reach their equilibrium swelling degree, as determined from the swelling studies. The concentration of 4% is close of that used for *in vitro* experiments for good comparison and also it assures the required administration dose, for a convenient solvent volume, to be safely delivered to rat.

The homogeneity of the theophylline distribution into polymeric matrices was evaluated by the near infrared chemical imaging (NIR-CI) technique. The nondestructive character and minimal sample preparation required, show the feasibility of this method technique which is used more to investigate samples with pharmaceutical application. NIR spectra were recorded on a SPECIM´S Ltd. SisuCHEMA NIR device controlled with Evince software package for processing the original image data. The system includes a Chemical Imaging Workstation for 1000-2500 nm NIR domains. The original image for each sample was taken with a NIR model spectral camera, respectively an imaging spectrograph type ImSpector N17E with 320 and 640 pixel spatial resolution at a rate of 60–350 Hz.

For the microscopic investigations the hydrogel samples loaded with theophylline were frozen by direct immersion in liquid nitrogen and fractured. After metallization with gold the sample examination was performed on a Quanta 3D Scanning Electron Microscope (USA). Magnification is given on the images.

2 2.3 *In vitro* and *in vivo* drug delivery

The *in vitro* release studies for theophylline have been performed by a standard dissolution test [28-30] carried out in conditions which mimic the gastrointestinal environment, using acidic buffer solution of pH 2.2 as dissolution medium. During the experiment, the temperature was maintained at 37±0.5ºC. The concentration of the drug was calculated based on calibration curves determined for the drug at specific maximum absorption wavelength. The measured concentration of drug in solution was 18 mg/100 mL. Aliquots of the medium of 1 mL were withdrawn at predetermined time intervals and analyzed at λ_{max} value of 271 nm, the wavelength characteristic for theophylline, using a HP 8450A UV–visible spectrophotometer. In order to maintain constant the measured drug concentration, the sample was carefully reintroduced in the circuit after analysis.

The drug release kinetics was evaluated with a semi-empirical equation (3) based on Korsmeyer-Peppas model, which is applied at the initial stages (approximately 60% fractional release). [31]

$$\frac{M_t}{M_1} = k_r t^{n\,r} \tag{3}$$

where M_t/M_1 represents the fraction of the drug released, M_t and M_1 are the absolute cumulative amount of drug released at time t and at infinite time respectively (in this case the maximum amount released in the experimental conditions used, at the plateau of the release curves), k_r is a constant incorporating the characteristics of the macromolecular drug loaded system and n_r is the diffusional exponent characteristic for the release mechanism.

In the equation above, a value of n ~ 0.5 indicates a Fickian diffusion mechanism of the drug from the hydrogel network, while a value 0.5 < n < 1 indicates an anomalous or non-Fickian behavior. When n = 1, a case II transport mechanism is involved with zero order kinetics, while n > 1 indicates a special case II transport mechanism [32].

The corresponding theophylline release profiles are represented through plots of the cumulative percentage of drug released versus time.

The theophylline release pharmacokinetic evaluation studies from CS/GA and CS/Na+MMT/GA hydrogels were conducted on healthy male Wistar rats weighing between 330 and 450 g, purchased from Cantacuzino Institute, Bucharest, Romania, using the retro-orbital sinus bleeding technique.

For the pharmacokinetic and *in vivo* release studies, the oral delivery was chosen, which the usual way for drug administration is. The animals were maintained in identical laboratory conditions as before, with free access to food and water. The raw theophylline and theophylline-loaded hydrogels were delivered by gastro-gavage as suspensions, in a dose of 15 mg/kg body weight for each rat [33].

The *in vivo* release study's protocol and methodology were detailed as well in our previous work [28,34]. The pharmacokinetic (PK) parameters such as maximum plasma concentration (C_{max}), time of maximum concentration (t_{max}) and plasma elimination half-life ($t_{1/2}$) were obtained directly from the plasma concentration–time plots. The area under the plasma concentration–time curve up to 72 h ($AUC_{0–72}$) was calculated using the linear trapezoidal rule. The relative bioavailability (test/reference ratios) of the chitosan based hydrogel formulations, compared to raw theophylline, was calculated as the ratio (AUC_{sample}/ $AUC_{theophylline}$) x 100. Each experiment was repeated four times and the results were represented as mean standard deviation.

3. RESULTS AND DISCUSSION

3.1 Characterization of Polymer Matrices Based on Chitosan

3.1.1 FT-IR-ATR spectroscopy

The spectral characteristics of the two systems based on chitosan were presented in Fig. 1 and Table 1 included in Appendix with additional information) where the main functional groups are assigned. The FT-IR spectrum of CS/Na^+MMT/GA looks very similar with that of pure chitosan except the additional bands appeared at 1708 and 1897 cm^{-1} which are characteristic to glutaraldehyde (GA) and also all the bands are wider proving that the crosslinking occurred.

It can be also remarked the shifts of the bands at 1027 (1065) cm^{-1}, 1987 cm^{-1} and 3286 cm^{-1}

assigned to carboxyl and ether groups, ammonium groups and intramolecular hydrogen-bonded hydroxyl groups, respectively which should be due to the interaction of chitosan with nanoclay as it was previously demonstrated by XDR study. Because of the hydrophilic and cationic structure of chitosan in acidic medium, this biopolymer has a good miscibility with montmorillonite (especially with Na^+MMT) and could easily intercalate into the interlayers by means of cationic exchange. After montmorillonite incorporation within CS, the basal plane of Na^+MMT from 2θ = 7.2º disappeared being substituted by a new peak at around 2θ~ 4- 5º [11]. The shift of the basal reflection of Na^+MMT to lower angle indicates the formation of an intercalated nanostructure, while the peak broadening and decreased intensity indicated the disordered intercalated or exfoliated structure. The enhanced thermal and mechanical properties [11] indicated also the formation of an intercalated structure between the chitosan and montmorillonite.

3.1.2 Swelling behavior

The swelling kinetic curves of the CS/GA and CS/Na^+MMT, at pH 2.2, are presented in Fig. 2.

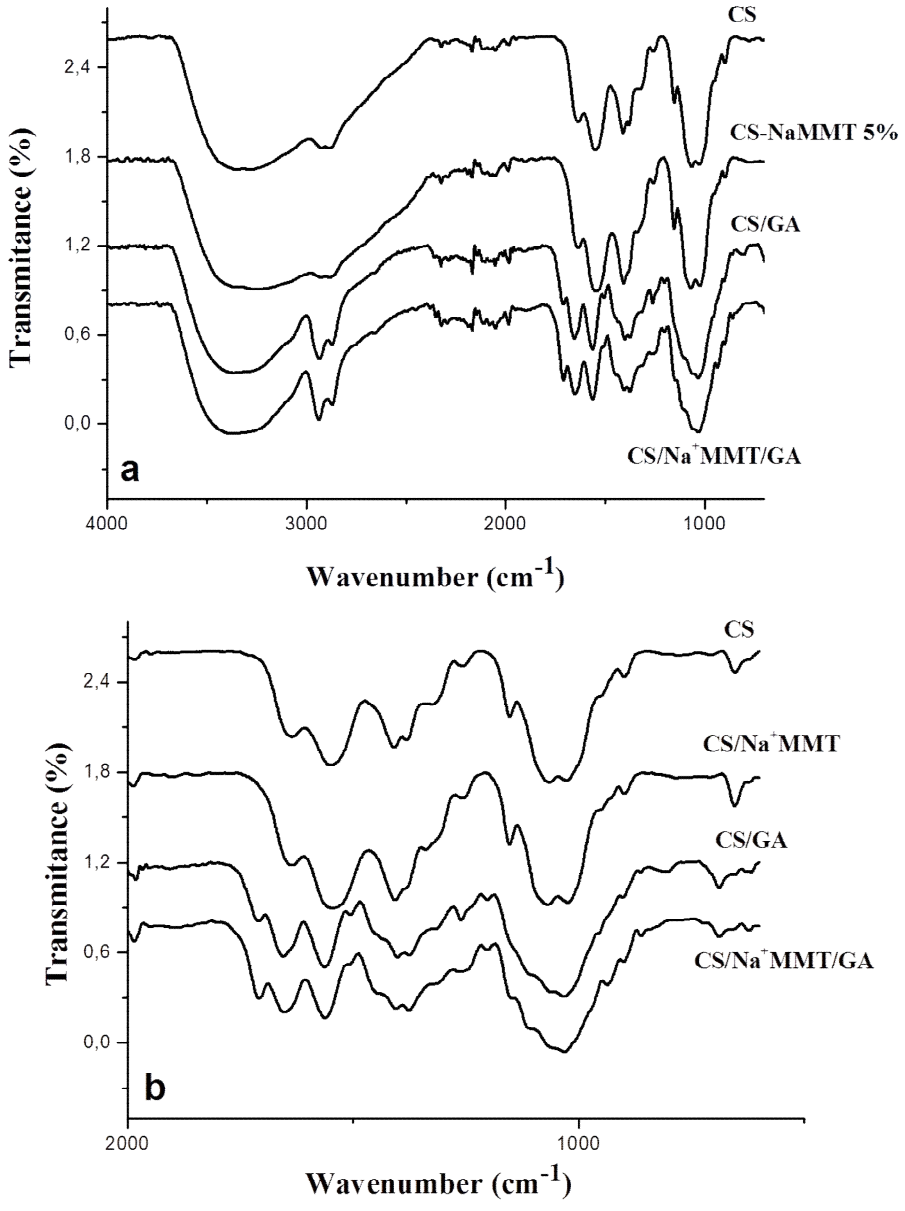

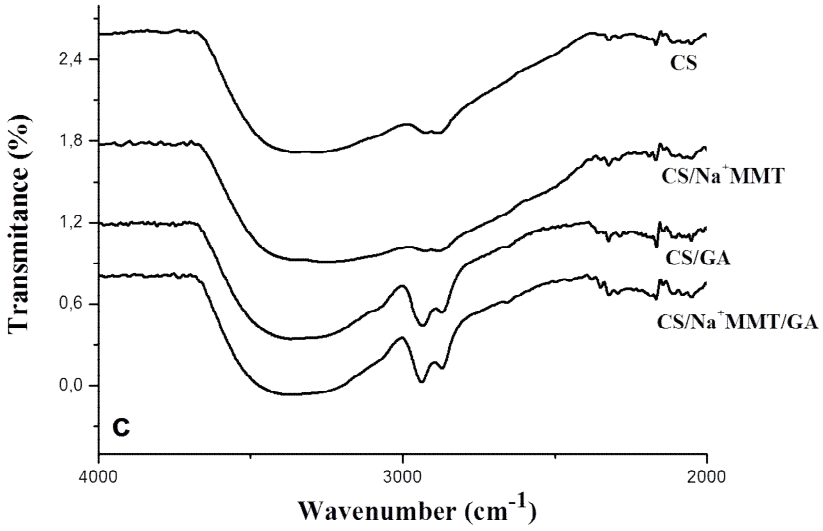

Fig. 1. FT-IR-ATR spectra of chitosan based hydrogels with 5 wt % Na^+MMT with and without crosskinking agent (GA): (a) whole spectrum, and different spectral regions (b) 925 – 2000; (c) 2000 – 4000 cm^{-1}

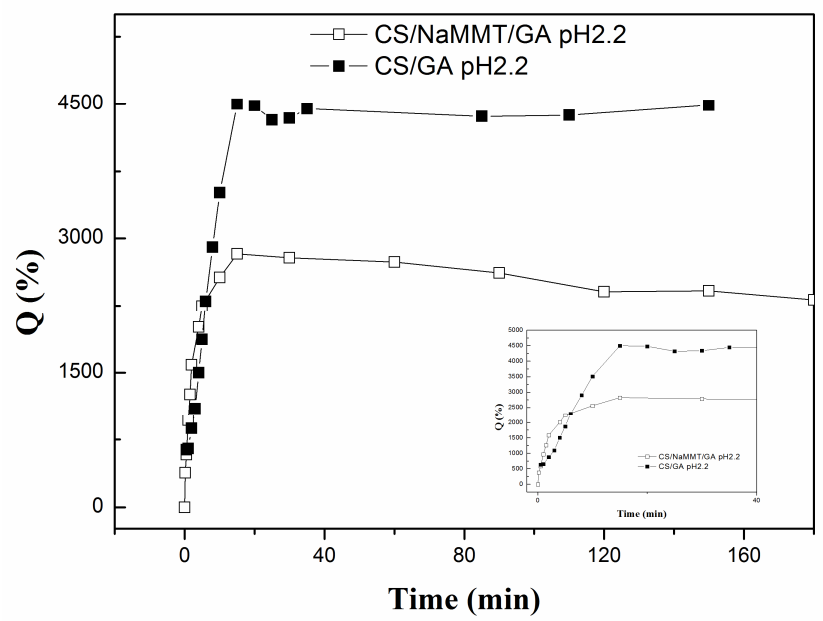

Fig. 2. Swelling kinetic curves of CS/GA and CS/Na^+MMT in acidic medium of pH 2.2

Hydrogels based on chitosan crosslinked with glutaraldehyde in a molar ratio of CS: GA 1: 0.33 showed a maximum swelling degree of about 4500% in acidic medium. By comparison the matrix containing chitosan and sodium montmorillonite and then crosslinked with GA had a swelling degree of about 3000% in similar conditions. After 1.5 hours the equilibrium is reached in both cases – Fig. 2. Both types of hydrogels containing chitosan and montmorillonite have a great ability of water absorption due to the porous structure of the sample as result of the lyophilisation. The montmorillonite particles played a filler role within the matrix as the polymeric system based on montmorillonite had a more dense structure like

and thus smaller pore sizes which cause a lower ability of adsorbing water inside the polymeric network.

The swelling kinetic parameters, k_{sw} and n_{sw}, have been determined by the graphic method applied to the swelling curves and the values are summarized in the Table 1, indicating an anomalous non-Fickian swelling mechanism. The value of the n_{sw} close to null confirmed that the swelling of both matrices is a complex process. The swelling kinetic parameters n_{sw} and k_{sw} took higher values for CS without sodium montmorillonite (n_{sw}=0.7; k_{sw}=38.43 $min^{-0.7}$)- values presented in Table 1- than those of CS/Na^+MMT/GA, therefore it can be concluded that the addition of clay induced a more time-controlled ability of retaining water within the polymer network.

Table 1. Swelling kinetic parameters for CS/GA and CS/Na^+MMT/GA

Sample	n_{sw}	k_{sw} (min^{-n})
CS/GA	0.7	38.43
CS/Na^+MMT/GA	0.4	26.84

It is well-known that the swelling kinetics of hydrogels can occurs either by a diffusion controlled (Fickian diffusion) phenomenon or relaxation controlled (non-Fickian process) [35]. The type of transport of the solvent into the hydrogel is indicated by n_{sw} from power law equation (eq 1) When the diffusion into the hydrogel is much faster than the relaxation of the polymer chains, the swelling kinetics tends to be diffusion controlled type and n_{sw} takes a limiting value of 0.5 (Fickian process). In the case of relaxation-controlled processes, n_{sw} is close to unity. When n_{sw} lies between 0.5 and 1, an anomalous transport is involved [36-38]. The non-Fickian kinetics is regarded as a coupled diffusion/polymer relaxation phenomena [39].

As n_{sw} for the hydrogels with montmorillonite was close to 0.5 the swelling process was rather a diffusion controlled while the value between 0.5 and 1 of the hydrogel CS/GA indicated an anomalous mechanism of swelling.

3.1.3 Degradation behavior of chitosan based matrices

Biodegradation can be regarded as a process in which the degradation products result from the action of microorganisms such as bacteria, fungi or algae. Biodegradation can be generally divided into two steps. The first step is depolymerization or random chain cleavage where the longer polymer chains undergo backbone scission into smaller oligomeric fragments under the action of enzymes secreted by microorganisms. The second step is mineralization, which occurs inside the cell in which small oligomeric fragments are converted to biomass, minerals and salts, water and gaseous substances such as carbon dioxide under aerobic environments and methane under anaerobic environments. Bio-based and biodegradable polymers (e.g. chitosan) and their composites may be broken down by the enzymes secreted by microorganisms. Once broken down to monomeric / oligomeric level, the polymer is used as the carbon source for the microorganism metabolism.

Chitosan can be degraded by enzymes which hydrolyse glucosamine–glucosamine, glucosamine–N-acetyl-glucosamine and N-acetyl-glucosamine–N-acetyl-glucosamine linkages [40]. Chemical degradation usually refers to acid catalyzed degradation i.e. in the stomach. The oxidation–reduction depolymerisation and free radical degradation [41] are unlikely to be a significant source or degradation *in vivo*. Therefore the enzymatic and chemical degradation of chitosan-based materials were investigated in the study.

3.1.3.1 Enzymatic degradation

The *in vitro* degradation was performed by treating the chitosan based materials, CS/Na+MMT/GA and CS/GA, with a solution of buffered phosphate at a pH 5.5 with 10 mL chitosanase solution having the activity of 4.78 U/ 100 mL (purchased from SigmaAldrich). The treated samples were kept further in oven under constant conditions at 37ºC. At different time intervals 1 mL from each type of sample was prelevated which content of N-acetyl D-glucosamine was analyzed by means of photocolorimetric method with potassium ferricianide developed by Horn et al. [42].

In Fig. 3 are represented the enzymatic degradation profiles of chitosan based materials, the concentration of N-acetyl D- glucosamine being calculated from the calibration curve. A low level of degradation under enzyme action could be observed in the case of chitosan montmorillonite sample without crosslinking agent of about 30-50% and the hydrogel without nanoclay suffered a rapid degradation of 80% in

the presence of chitosanase. The degradation mechanism is slow and depends on nanoclay presence which acts as a barrier for enzyme action and also probably due to the more pronounced interactions of it with chitosan.

3.1.3.2 Chemical degradation

The chemical degradation was followed in acidic solutions at pH 2.2 by exposing the two types of samples and monitoring the weight variation periodically during 72 hours. The degradation profiles were plotted in Fig. 4 as weight loss vs. time.

The addition of clay into the polymer matrix is even more visible by analyzing the weight loss profile of the hybrid hydrogel under the action of acidic medium. The loaded montmorillonite chitosan hydrogels having a more compact structure is less susceptible to acidic erosion, being more chemically stable. By comparison the matrix without nanoclay has a porous like structure which is in acidic solution much freely entered inside the hydrogel network leading to faster degradation process or to the partially chitosan dissolution.

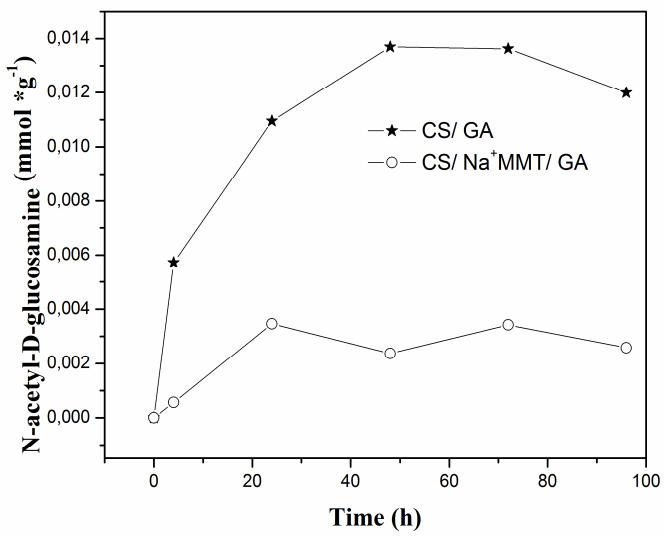

Fig. 3. *In vitro* degradation profile of chitosan based materials at pH 5.5 under the action of chitosanase

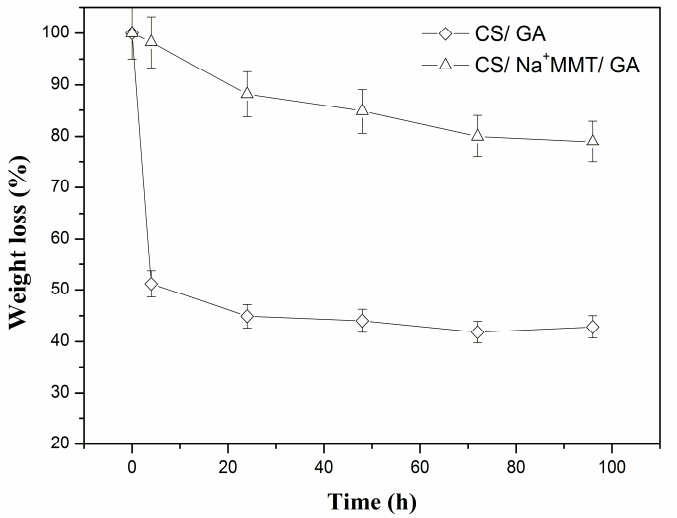

Fig. 4. Weight loss profile of chitosan based hydrogels at pH 2.2

The degradation products resulted from both enzymatic and acidic actions were evidenced also by means of ATR -FT-IR spectroscopy by comparison of the characteristic vibration bands of functional groups of the chitosan based materials which were degraded by both ways via enzyme and acidic medium – Figs. 5a and b.

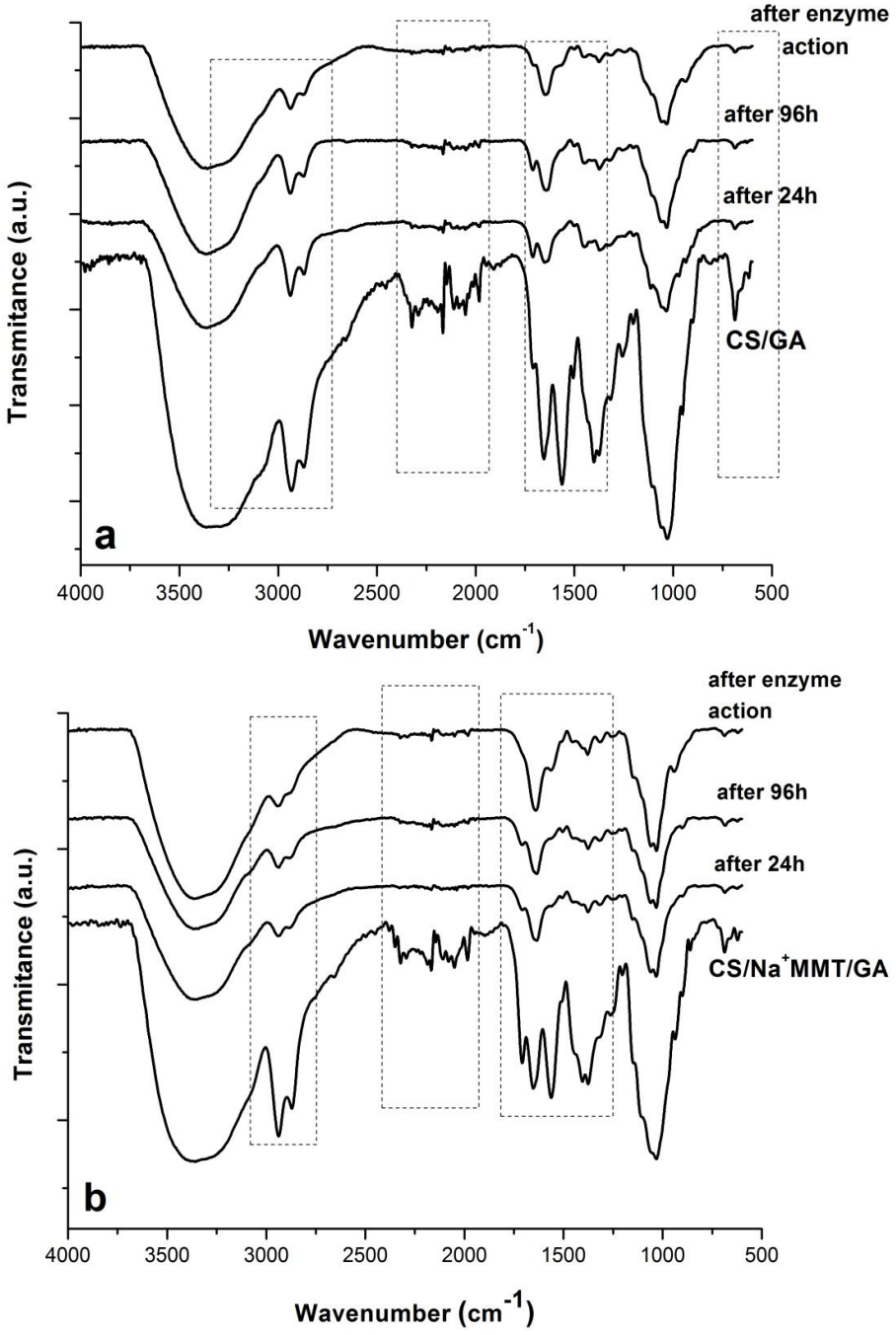

Fig. 5. ATR-FT-IR spectra of chitosan based samples degraded by chemically and enzymatically methods after 96 hours from the beginning of degradation (a) hydrogels of CS/GA (b) hydrogels of CS/Na^+MMT/GA

The structural changes as result of degradation were observed by using FT-IR spectra. The degradation process was evidenced based on the intensity of the peaks, position of the characteristic bands of the functional groups susceptible to degradation.

The main functional groups susceptible to degradation which were considered within the degradation analysis are listed below:

- 3450 - OH group
- 3360- NH group stretching vibration
- 2920, 2880, 2430, and 1320- symmetric or asymmetric CH_2 stretching vibration attributed to pyranose ring
- 1730 - carbonyl group vibration
- 1655 - C=O in amide group [I amide band]
- 1560 - NH- bending vibration in amide group
- 1590 – NH_2 in amine group
- 1380 - CH's in amide group
- 1150-1040- C-O-C- in glycosidic linkage

As it can be observed in Fig. 6 the main functional groups susceptible to degradation are OH bands, evidenced at 2900-2880 cm^{-1} and NH_2 bands from 1650 to 3400 cm^{-1}.

The decrease of the intensity of the characteristic bands for amide I and II indicates the decrease of the desacetylation degree (DD) both in enzymatic and chemical degradation Table 2. The values for desacetylation degrees, calculated according to the method developed initially by Roberts [43].

The characteristic bands of OH bonds and those ones characteristic to the chemical crosslinking with glutaraldehyde from 2900-2880 cm^{-1} and the bands from region 2300 -1700 cm^{-1} disappeared once the degradation is taking place. Also, the characteristic bands of polysaccharide structure from 900-1000 cm^{-1}, are modified in the way of the decreased intensity and appearance of a new band at 932 and 944 cm^{-1} for CS/GA and 900 cm^{-1} for CS/Na^{+}MMT/GA degraded in the presence of chitosanase. This is indicating the formation of the chito-oligosacharide with lower molecular weight [44].

3.1.4 Cell viability, toxicity and biocompatibility studies

3.1.4.1 Cell viability assays

The hydrogels based on chitosan crosslinked with glutaraldehyde with and without nanoparticles exhibit potential utility for many biomedical applications due to their gel state, antimicrobial activity, mucoadhesivity and biocompatibility of chitosan. Cells viability was calculated by comparison with control samples (*S. pombe* cultivated in absence of polymers), considered to be 100% viable cells. The effect of hydrogels on cell growth was evaluated by MTT test, a rapid and economical assay for measurement of cellular viability. In Fig. 6 is presented the cell viability as results of chemiluminescence assays to detect the viability of *S. pombe* after 4 h cultivation. The chitosan hydrogels exhibited cell viability comparable with the control sample which means a good biocompatibility and didn't show inhibitory effect on the cell's growth; moreover MMT seems to improve this characteristic slightly.

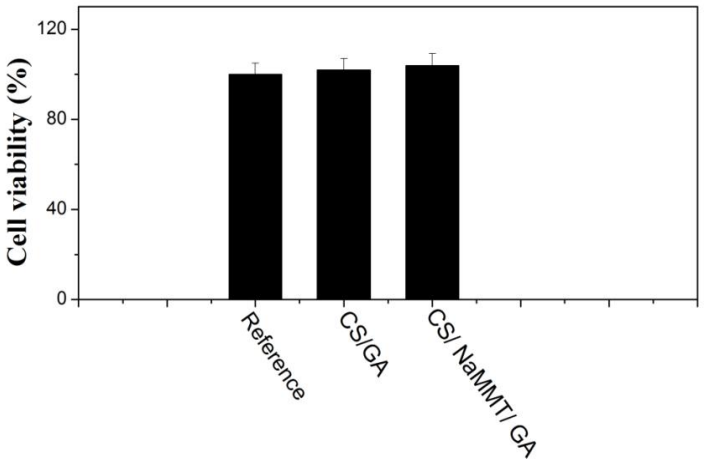

Fig. 6. *S. pombe* viability detected by chemiluminescence assay after 4h cultivation

3.1.4.2 Hemocompatibility

The method is based on measurement of the hemoglobin released by hemolysis. Hemolysis is regarded as a special significant screening test, once it provides quantification of small levels of plasma hemoglobin, which may not be measurable under *in vivo* conditions. Table 3 summarizes the values of hemolysis obtained for the chitosan hydrogels. As reported in literature [45] it is not possible to define a universal level of acceptable or unacceptable amounts of hemolysis. Although by definition a blood compatible material should be non-hemolytic, in practice several medical devices cause hemolysis. This means that when such hemolytic effect takes place, it is important to make sure that clinical benefits overcome the risks and that the values of hemolysis are within acceptable limits. According to ASTM standard, [46] the materials can be classified in three different categories according to their hemolytic index (hemolysis %). Materials with percentages of hemolysis over 5% are considered hemolytic; while the ones with hemolytic index between 5% and 2% are classified as slightly hemolytic. Finally, when the material presents a hemolysis percentage below 2% it is considered as a non-hemolytic material. The data of Table 3 indicated a hemolysis degree of both samples less than 0.2% therefore they are not hemolytic.

3.1.4.3 Toxicity tests of CS/Na^+MMT/GA

The first test consisted on intraperitoneal (i.p.) administration of a single dose of 2000 mg hydrogel suspension per kg [33] body at a mouse, of each composition. Because the mice survived up to 2 weeks after administration, four other mice were injected for each composition, and their survival was assessed. It was found that all mice survived 14 days after i.p. administration of hydrogel suspensions. No behavioral or physical changes such as abdominal swelling were observed in treated mice following injection or on subsequent days. Throughout the study period, animals showed no signs of peritonitis, lethargy, muscle loss, dehydration or anorexia, symptoms which are associated with animal toxicity [47].

The acute toxicity of a 5000 mg/kg [33] body dose was tested according to OECD guidelines [48]. Due to technical problems occurred at administration of the solutions with such a high concentration, one single dose of 3200 mg kg body was tested. It was found that after a single dose of 3200 mg /kg body of hydrogel suspension intra-peritoneal administered to mice, for each composition, they survived 14 days after administration. *It has been concluded that the LD50 for CS/Na^+MMT/GA hydrogels, after i.p. administration as suspensions, is bigger than 3200 mg kg body, showing their nontoxicity.*

3.1.4.4 Biocompatibility of CS/Na^+MMT/GA hydrogels

The *in vivo* biocompatibility of CS/Na^+MMT/GA hydrogels was examined during 14 consecutive days after i.p. injection of gel suspensions at mice, following the effects on hematological and immune system parameters comparatively with a control group of mice, which received physiological serum (Table 4).

Table 2. Desacetylation degree of the chitosan based matrices calculated from FT-IR spectra

DD of CS/GA (%)	DD of CS/Na^+MMT/GA (%)	Enzymatic degradation		Chemical degradation	
		DD of CS/GA (%)	DD of CS/Na^+MMT/GA (%)	DD of CS/GA (%)	DD of CS/Na^+MMT/GA (%)
65	65	44	45	38	58

Table 3. Hemolysis results for the chitosan base hydrogels

Sample	A415	A380	A470	Biomaterial concentration	Hemolysis degree (%)
CS/GA	0.454	0.178	0.129	0.488	0.114
R^+	0.828	0.217	0.059	1.122	
R^-	0.371	0.175	0.120	0.362	
CS/Na^+MMT/GA	1.064	0.355	0.155	0.598	0.178
R^+	0.283	0.167	0.076	1.437	
R^-	0.076	0.122	0.122	0.341	

R^+, R^-; positive and negative reference samples

Table 4. Hematological and immune systems parameters (mean standard deviation STD) at Mice i.p. Injected with CS/Na$^+$MMT/GA suspensions

Hematological parameter	Control mice group	Tested mice groups Mice group intraperitoneal injected with CS/Na$^+$MMT/GA solution
White blood cells (x 10^9/L)	5.64±0.13	5.6±0.11
Polymorphonuclear cells (PMN) (x 10^9/L)	1.51±0.06	1.44±0.09
Lymphocytes (x 10^9/L))	3.68±0.11	3.7±0.1
Monocytes (x 10^9/L)	0.35±0.05	0.35±0.05
Eosinophils(x 10^9/L)	0.04±0.02	0.05±0.01
Basophils (x 10^9/L)	0.05±0.03	0.06±0.02
Polymorphonuclear cells (PMN) (%)	26.8±0.97	25.7±1.49
Lymphocyte (%)	65.3±1.05	66.08±1.44
Monocytes (%)	6.23±0.71	6.27±0.74
Eosinophils (%)	0.78±0.36	0.79±0.2
Basophils (%)	0.93±0.47	1.11±0.3
Red blood cells (x 10^9/L)	9.39±0.06	9.4±0.06
Hemoglobinlevel (g/dL)	11.5±0.05	11.48±0.19
Hematocrit level (%)	41.0±0.04	41.27±0.41
NBT test (%)	13.8±0.75	13.83±0.75
Platelets (x 10^9/L)	253±38.8	252.99± 8.5
Immune system parameter		
Serum opsonic capacity (S. aureus ×1000/mL)	771.7±58.4	768.33±54.92
Phagocytic capacity of peritoneal macrophages (S. aureus ×1000/mL)	716.7±51.6	715±52.44
Bactericidal capacity of peritoneal macrophages (S. aureus ×1000/mL)	696.7±8.2	696.67±5.16
Splenic T lymphocytes (%)	12.5±0.55	12.67±0.52
TGP (UI/l)	23.17±1.17	36±0.84
TGO (UI/l)	73.33±1.75	84.83±1.7
LDH (UI/l)	497.5±3.33	500.17±1.33

Clinical chemistry and hematology data are of great importance to determine the effects induced on the body by the tested hydrogel matrices.

The values of hematology parameters such as white blood cells (WBC), red blood cells (RBC), platelets (PLT), hemoglobin level (HGB) concentration, hematocrit level showed no significant variations between mice groups treated with CS/Na$^+$MMT/GA hydrogels compared with control mice group, being in the range of normal limits reported for healthy mice [49]. Statistical analysis revealed no significant influence of the studied compounds on the neutrophils phagocytic capacity, on the phagocytosis activity of immune cells, serum opsonic capacity, phagocytosis and bactericidal capacities of peritoneal macrophages, splenic lymphocytes with rosetting capacity of tested mice compared to control group, after 14 days of testing.

As it concerns the clinical biochemistry parameters, a statistically significant increase of ALT and AST values was observed in the experimental groups compared with the control mice group after 14 days of testing – Table 4, but the values are in the range of normal limits. There was no significant effect on LD levels in case of mice injected with CS/Na+MMT/GA hydrogel suspensions compared with that obtained for control mice group. Based on the toxicity and biocompatibility results it can be considered that the injected CS/Na$^+$MMT/GA hydrogels are nontoxic and did not produce any significant changes in the hematology of tested rats and had no hepato-toxicity effect. All presented results indicate a good biocompatibility of CS/Na$^+$MMT/GA hydrogels with living tissues, so they could be considered as potential carriers for controlled drug delivery and other biomedical applications (e.g. wound dressing tissue engineering, etc.).

3.2 Characterization of Drug Loaded Matrices

3.2.1 Near infrared chemical imaging (NIR-CI)

Theophylline distribution into CS/GA and CS/Na^+MMT/GA hydrogels was evaluated by the near infrared chemical imaging (NIR-CI) technique. The prediction of drug loading degree was evaluated based the new near infrared chemical imaging maps. The chemical imaging provides a simple method for evaluating the spatial drug distribution.

The non-destructive character and minimal sample preparation required, show the feasibility of this technique which is used more to investigate samples with pharmaceutical applications. Both PLS-DA (partial least squares-discriminate analysis) and PCA (principal component analysis) models were used to determine the homogeneity and prediction of the two components, namely the drug and polymeric matrix. PLS-DA model based on multivariate inverse least squares discrimination method is used by Evince to classify the components. This could be achieved because of these two models based on mathematical processing.

Assigning a color for each component, class of principal components, allows visual assessment of the degree of homogeneity of the components. As noted with a value between 0 and 1 of the same original component facilitated obtaining quantitative information. For the first component value 1 represents available percentage of 100% and the value tends to zero when there is an unknown structure. It is appreciated the correct information available upon the cube of information can be extracted. The final images have for every pixel a complete spectrum that includes contributions from all the chemical components present in system.

The images of Fig. 7 correspond to the PLS-DA model for CS/GA and CS/Na^+MMT/GA hydrogels. A visibly uniform distribution, corresponding to a high homogeneity degree of the drug in the CS-based hydrogel matrix was observed. Based on PLS-DA prediction, a drug loading up to 66% into the CS/Na^+MMT/GA hydrogel and 78.6% into CS/GA hydrogel was found from theophylline loaded amount. In Fig. 8 are shown the NIR spectra of theophylline, for the two systems in the full range of the near infrared region with an air background. The obviously overlap between the polymers and theophylline bands in near infrared region empower for the use a multivariate regression for the simultaneous determination of drug content in samples.

New bands are present within the spectra of polymers containing theophylline, specifically at 1438 and 1515- 1530 cm^{-1} which might be attributed to the new interactions between active substance and polymeric materials within N-H vibration domain. Also the bands vibrations corresponding to the C-N- C stretch overtone are present at 2475 cm^{-1} in the spectra of the polymer loaded with theophylline as well as the spectrum of theophylline confirming the presence of drug within the polymer network and confirming also FT-IR data. Additional information regarding the assignments of the peaks is included in Table 2 from Appendix.

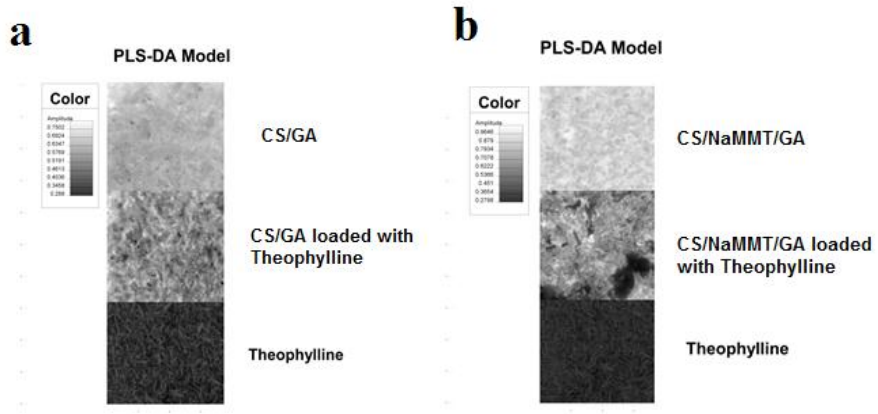

Fig. 7. PLS-DA model for (a) CS/GA (b) CS/Na+MMT/GA hydrogels

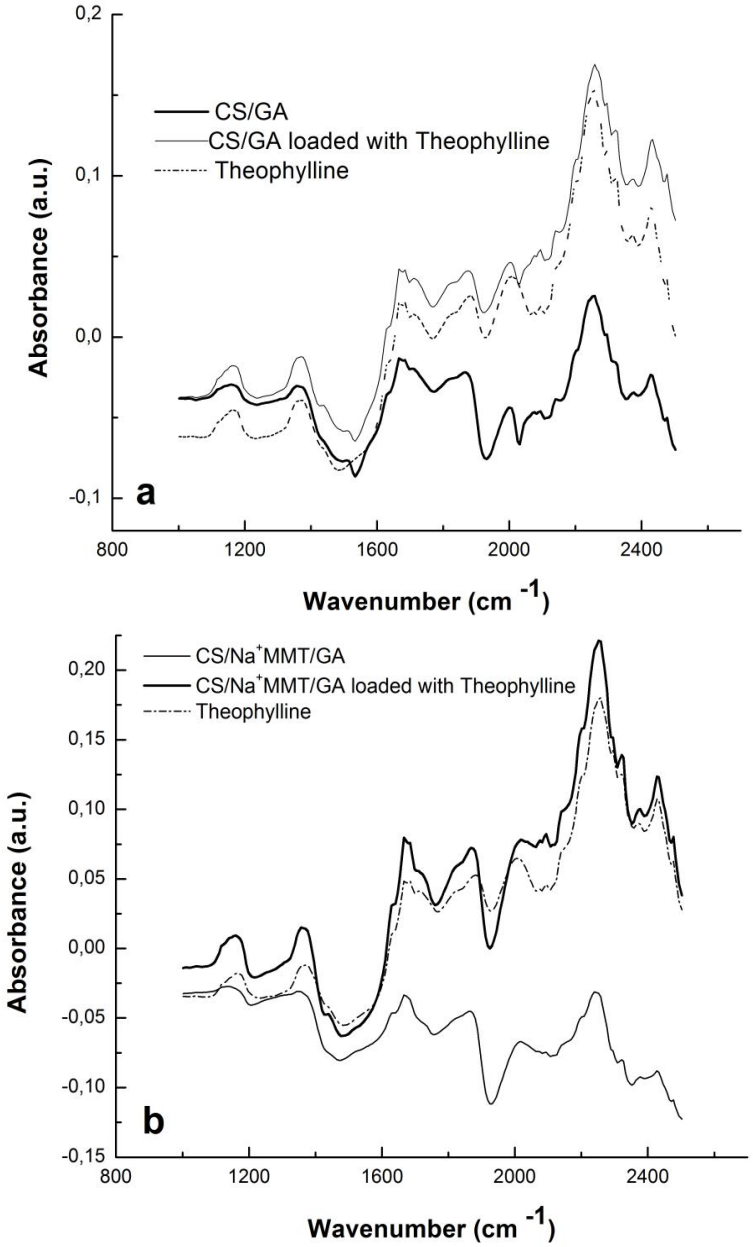

Fig. 8. Near-IR reflectance spectra of the unloaded and theophylline loaded (a) CS/GA (b) CS/Na^+MMT/GA hydrogels

3.2.2 Scanning electron microscopy

The SEM images (Figs. 9a - f) confirmed that theophylline was dispersed within the polymeric matrices as stick-shaped microparticles, and relative uniform distribution being identified in accordance with NIR results. It can be noticed that the drug microparticles, with various dimensions in the range 8 to 46 μm were better dispersed within the polymeric networks containing silicates layers of Na^+MMT, the matrix being more dense and homogenous, while in the sample without clay nanoparticles, the theophylline seems to agglomerate in clusters and alternating with CS/GA hydrogel structures. The SEM images confirmed the NIR-CI results regarding the uniform distribution of theophylline within the polymer matrices.

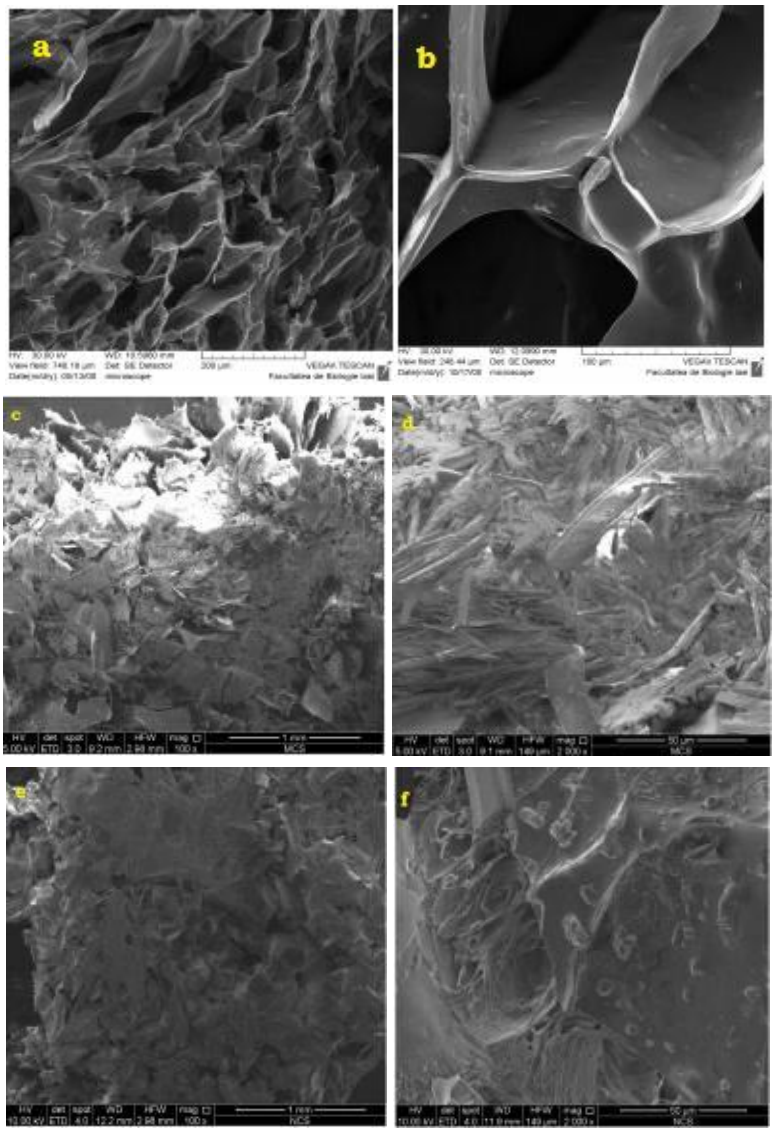

Fig. 9. SEM micrographs of hydrogel samples of (a) CS/GA (b) CS/Na+MMT/GA; (c), (d) CS/GA/ Theophylline; (e), (f) CS/Na^+MMT/GA / theophylline hydrogels. Magnification is given on pictures

3.2.3 Thermal characterization

Thermal stability and information related to the degradation steps of the both polymeric systems unloaded and loaded with theophylline were assessed by analyzing the weight loss from 20 to 700ºC (TG curves) as well as the derivative DTG curves - Fig. 10. The information achieved regarding the thermal decomposition is important in terms of determination of the temperature range, in which the active substance is stable both in its structure and pharmaco-therapeutic action.

All the samples recorded a thermal event at 45–100ºC being attributed to the loss of hydration. Pure chitosan was stable until higher temperatures (over 150ºC), the obtained data being in accordance with those found by other authors [50-54] showing a single degradation stage within a temperature range of 249–302–476ºC, whereas the system based on CS cross-linked with glutaraldehyde showed two degradation steps. Temperature ranges determined from TG and DTG curves are summarized in Table 3 and added as supplementary information in Appendix.

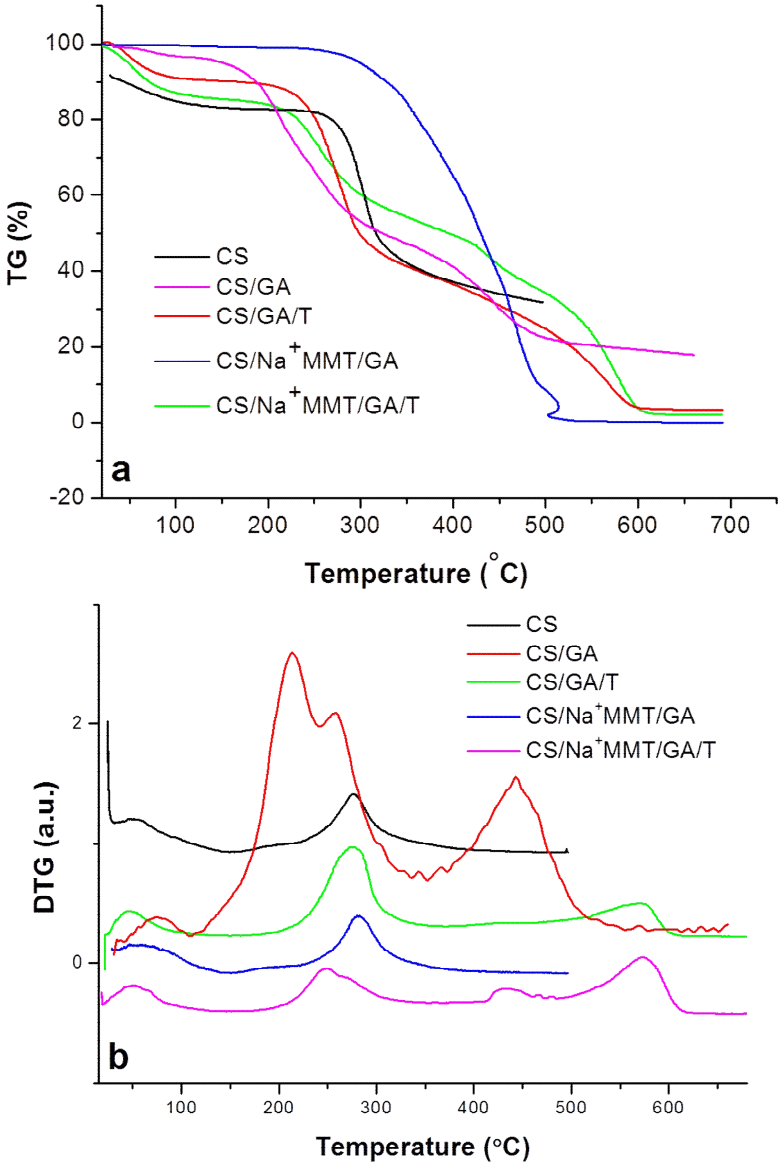

Fig. 10. The thermo-gravimetric (a) and DTG (b) curves of CS/ GA and CS/Na+MMT/GA loaded with theophylline (T) TG results

As shown in the Fig. 10b, addition of theophylline within the polymeric matrix with and without clay influences significantly the thermal behavior of the systems. As described by Wesolowski et al. [55,56] theophylline suffers a two and three-stage decomposition processes excepting the water removal.

As the melting point of theophylline was reported as being around 270ºC [57], the peak recorded at around 273ºC for CS/GA/T and 266ºC for CS/Na$^+$MMT/GA/T are assigned to the melting process of theophylline connected with a change of phase transformation or a polymorphic change. A second stage of decomposition attributed to the theophylline degradation was recorded about 429ºC, where a lower and wider endothermic peak in DTG curve is observed In the case of CS/GA/T is almost invisible. This stage can be connected with the vaporization of the liquid phase (melted drug) being related to a heat of evaporation. The process of evaporation occurs frequently with decomposition of the melted compound. In the third stage, over 500ºC, as a result of further increase of temperature, the products of decomposition are subject to final

destruction combined with complete deflagration of the carbonated rests.

Regarding the polymeric matrices without theophylline, the effect of crosslinking is evidenced by the thermal event around 400ºC, the obtained results being correlated with the study performed by Poon et al. [58] as concerning thermal stability of chitosan crosslinked with glutaraldehyde. A synergetic effect of clay and active substance is observed in the case of mass loss as the temperature increase of the matrix CS/Na^+MMT/GA/T conferring higher thermal stability as compared with the other matrices.

3.3 Study of the *in vitro* Drug Delivery Kinetics of Theophylline

As chitosan and chitosan based materials are rather soluble in acidic medium, the *in vitro* study of the drug delivery ability of the nanocomposites based on chitosan and clay was performed in acidic medium at pH 2.2 simulating the physiological medium from stomach and a temperature of 37ºC. Loading of the drug into the chitosan matrices were performed taking into account the maximum amount of liquid absorbed by the matrices at pH 2.2 and 37ºC, value obtained from swelling profile (Fig. 3).

The release profiles of theophylline from CS/Na^+MMT/GA hydrogel are shown in Fig. 11. It was studied the time-dependence of the percent theophylline released from the hydrogels based on chitosan of CS/GA and CS/Na^+MMT/ GA; the hydrogels were loaded with active substance based on the adsorption and absorption ability of the chitosan matrices. The amount released in time was compared with the initial loaded amount of drug, the result being represented in released percentages. A lower amount of drug was released from CS / GA without any clay in the composition, more specifically; the maximum amount of theophylline released from CS/GA hydrogel was 86% in respect to the loaded amount of drug within the matrix. The prolonged release of theophylline from CS/Na^+MMT/GA was observed, the time to reach the maximum amount released being reached after 7 hours from the beginning of dissolution test and the half release time value of 190 min. Analyzing the matrix without crosslinking agent (i.e. glutaraldehyde) and its abilities as drug vehicle [20,21] by comparison with the hydrogel containing sodium montmorillonite it can be remarked that the prolonged release profile of CS/Na^+MMT/GA as well as the slower release rate in time can be due to the presence of sodium montmorillonite which retarded the rate of theophylline release.

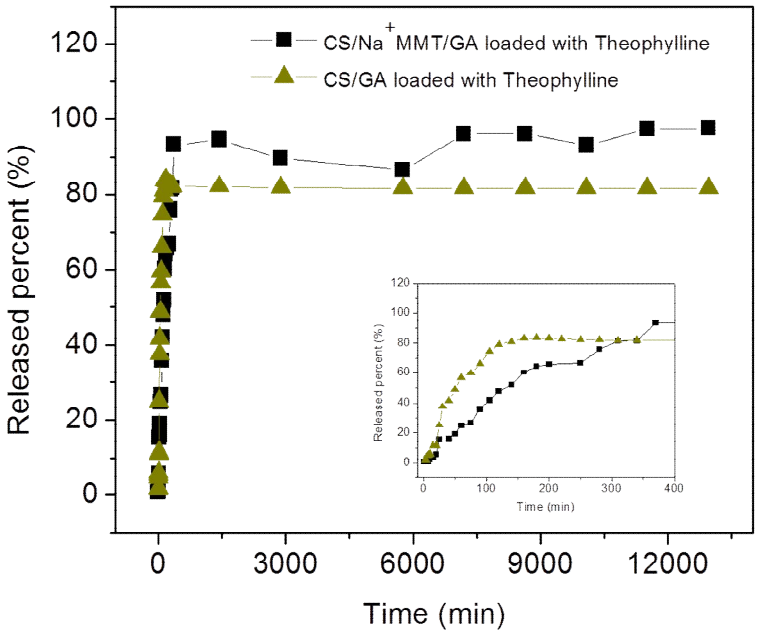

Fig. 11. Kinetic release profile theophylline from CS/GA and hybrid chitosan- montmorillonite hydrogels at pH 2.2 and 37ºC

As also shown in Fig. 11, the hybrid hydrogels of chitosan loaded with active substances (i.e. theophylline) had the ability of releasing under simulated physiological condition approximately 98% from loaded theophylline in the case of polymeric matrices containing montmorillonite while the chitosan hydrogel cross-linked had the ability of releasing of 86% of theophylline from the total loaded amount.

The kinetic analysis of the *in vitro* theophylline release mechanism was done by applying the general kinetic equation which allows the calculation of the parameter, n_r, and to obtain information related with the release mechanism type – eq. 4. By logarithmic transformation of equation (4) and applying the model of monitoring the first 60% of the theophylline release process [59]. The exponent n_r took values close to 1 for the release of the theophylline from CS/GA hydrogel [21] showing a non-Fickian release (anomalous transport) mechanism while for the theophylline release from CS/Na^+MMT/GA, nr was higher than 1, corresponding to a relaxation-controlled delivery (zero order) type (Table 5), which is known as more favorable kinetics for drug delivery.

The constant k_r decreased with the addition of clay within the chitosan based matrix from 60* 10^{-3} min -1.07 to 0.4 * 10^{-3} $min^{-1.6}$ (Table 5). This indicated that the release of theophylline from the CS/Na^+MMT/GA was retarded. A sustained release particulate system based on ofloxacin (OFL)/montmorillonite (MMT)/chitosan (CTS) nanocomposite microspheres was obtained also by Hua et al. [60]. By incorporating MMT into the nanocomposite microspheres the burst release effect observed in the case of release of theophylline from CS/GA hydrogels was significantly reduced, both half release time and time to reach maximum amount released increasing significantly –see Fig. 11- insert.

3.4 Study of the *In vivo* Drug Delivery Kinetics of Theophylline

The *in vivo* release of raw theophylline and theophylline loaded within the two types of matrices based chitosan i.e. CS/GA and CS/Na^+MMT/GA were studied. The mean plasma theophylline concentration versus time curves after a single oral dose are represented in Fig. 12 and mean values of pharmacokinetic parameters (C_{max}, $t_{1/2}$, and $AUC_{0–72}$) are summarized in Table 6.

Pure theophylline was detected in plasma within the first hour after its administration in rats. The mean plasma level of raw theophylline was recorded at a C_{max} value of 7.1 μg/mL achieved at a t_{max} of 1.5 h and the elimination half-life ($t_{1/2}$) of about 2.5 h, which indicated a fast absorption of pure theophylline, results data which are consistent with previous studies [28].

Table 5. The kinetic parameters and release characteristics of theophylline from CS hydrogels evaluated according to Korsmeyer–Peppas equation

Sample	Half release time (min)	Time to reach maximum amount released (min)	Maximum released amount (%)	Korsmeyer–Peppas equation		
				n_r	$k_r * 10^3 (min^{-nr})$	R
CS/GA	17	250	86	1.07	60	0.97
CS/Na^+MMT/GA	120	370	93	1.6	0.4	0.97

Table 6. Pharmacokinetic parameters obtained for raw theophylline and theophylline loaded CS/GA and CA/Na^+MMT/GA hydrogels

Pharmacokinetic parameter	Theophylline (THP)	CS/GA	CS- Na^+MMT /GA
t_{max} (h)	1.5	5	4
$t_{1/2}$	2.5	12	14
C_{max} (μg/mL)	7,1	6.7	5.87
AUC_{0-72} (μg h/mL)	41.52	134	127
Relative bioavailability (%)	-	322	306

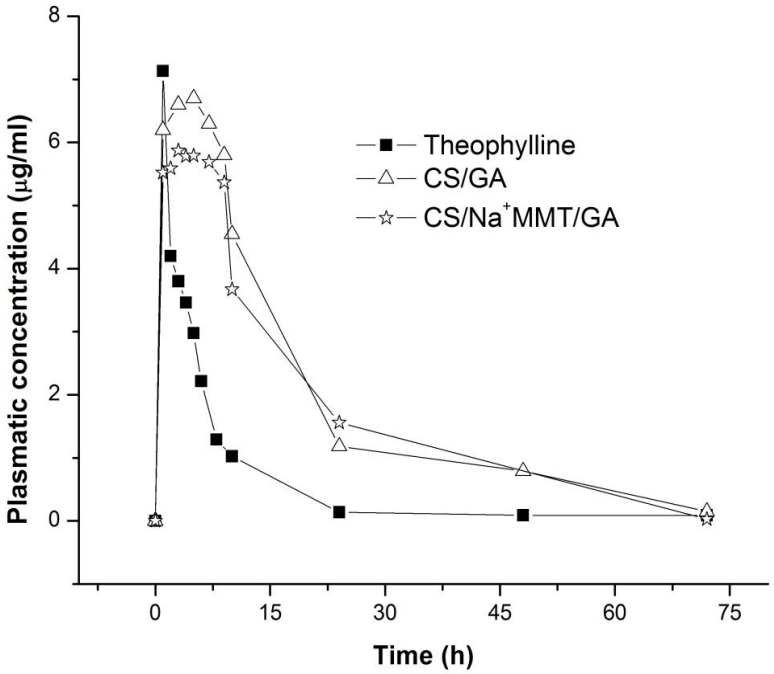

Fig. 12. Plasma theophylline concentration versus time. Each point is presented as mean±SD, n=4.

The *in vivo* release profiles showed the sustained release of theophylline loaded in CS/GA and CS/Na^+MMT/GA formulations compared with raw theophylline which is removed from the body in the first 17 h from administration. The prolonged release behavior of theophylline loaded in CS/GA and CS/Na^+MMT/GA formulations were proved by the presence of drug recorded up to 50 h from administration time. The evaluated pharmacokinetic parameters are given in Table 6.

As listed in the Table 6, theophylline release profile showed higher values for the pharmacokinetic parameters. This is translated by a retarded release of the drug as the matrices were more complex and played their role in the drug protection against fast release. The *in vivo* profile of theophylline delivery was not consistently different by incorporating montmorilonite within the chitosan network. The major achievement was the improvement of the half-release time ($t_{1/2}$) from from 12 to 14 hours indicating the possibility of reducing the administration frequency of the drug, with a prolonged action time, which is beneficial to the patient.

The relative bioavailablility of the drug did not show significant relevance, theophylline having high bioavailability in both cases by using a simple croslinked matrix of chitosan and a more complex system like CS/Na^+MMT/GA.

4. CONCLUSION

Matrices based on chitosan cross-linked with glutaraldehyde with and without montmorillonite nanoparticles were studied in terms of their application as drug delivery systems. Physical chemical characterizations were used to evidence the components and the distribution of the drug inside the matrices. The chitosan-based hydrogel systems showed a good biocompatibility with living tissues, so they can be considered as potential carriers for controlled drug delivery. Theophylline release profiles showed higher values for the pharmacokinetic parameters indicating a retarded release of the drug as the matrices were more complex and played their role in the drug protection against fast release. The *in vivo* profile of theophylline delivery was not consistently different by incorporating montmorillonite within the chitosan network. The major achievement was the improvement of the half-release time ($t_{1/2}$) from from 12 to 14 hours, indicating the possibility of reducing the dosing frequency, but with prolonged action time, which is beneficial to the patient.

CONSENT

It is not applicable.

ETHICAL APPROVAL

All authors hereby declare that "Principles of laboratory animal care" (NIH publication No. 85-23, revised 1985) were followed, as well as specific national laws where applicable. All experiments have been examined and approved by the Animal Research Ethics Committee from "Gr. T. Popa" University of Medicine and Pharmacy of Iasi, Romania (official paper no. 15559/21.09.2010) in rigorous accordance with international ethical regulations on laboratory animal work approved by the animal research ethics committee

ACKNOWLEDGEMENTS

The research leading to these results received financial support from COST Action FA0904 by the STSM grant (01/11/2010 – 30/11/2010) ECOST-STSM-FA0904-011110-003378A and research grants of the Romanian ANCS – UEFISCDI 164/2012 BIONANOMED.

COMPETING INTERESTS

Authors have declared that no competing interests exist.

REFERENCES

1. Felt O, Buri P, Gurny R. Chitosan: A unique polysaccharide for drug delivery. Informa Healthcare. 1998;24:979-993. Accessed 27 January 2015. Available:http://informahealthcare.com/doi/abs/10.3109/03639049809089942
2. Agnihotri SA, Mallikarjuna NN, Aminabhavi TM. Recent advances on chitosan-based micro- and nanoparticles in drug delivery. J Control Release. 2004;100:5-28.
3. Patel MP, Patel RR, Patel JK. Chitosan mediated targeted drug delivery system: A review. J Pharm Pharm Sci. 2010;13(4):536-57.
4. Katti KS, Katti DR, Dash R. Synthesis and characterization of a novel chitosan/ montmorillonite/hydroxyapatite nano-nanocomposite for bone tissue engineering. Biomed Mater. 2008;3(3):034122.
5. Haroun AA, Gamal-Eldeen A, Harding DRK. Preparation, characterization and in vitro biological study of biomimetic three-dimensional gelatin – montmorillonite/cellulose scaffold for tissue engineering. J Mater Sci Mate Med. 2009;20:2527–40.
6. Verma D, Katti KS, Katti DR. Osteoblast adhesion, proliferation and growth on polyelectrolyte complex – hydroxyapatite nanonanonanocomposites. Phil Trans R Soc A. 2010;368:2083-97.
7. Pongjanyakul T, Priprem A, Puttipipatkhachorn S. Investigation of novel alginate-magnesium aluminum silicate micronanocomposite films for modified-release tablets. J Control Release. 2005;107:343-56.
8. Wang X, Du Y, Luo J, Lin B, Kennedy JF. Chitosan/organic rectorite films: Structure, characteristic and drug delivery behavior. Carbohydr Polym. 2007;69:41-9.
9. Wang X, Du YM, Luo J. Biopolymer/montmorillonite nano nanocomposite: Preparation, drug-controlled release property and cytotoxicity. Nanotechnology. 2008;19: 065707.
10. Darder M, Colilla M, Ruiz-Hitzky E. Biopolymer–clay nanonanonanocomposites based on chitosan intercalated in montmorillonite. Chem Mater. 2003;15(20):3774-80.
11. Cheaburu CN, Vasile C, Duraccio D, Cimmino S. Characterisation of the Chitosan/layered silicate nanocomposites. Solid State Phenomena. 2009;151:123-8.
12. Wang S, Shen L, Tong YJ, Chen L, Phang IY, Lim PQ, Liu TX. Biopolymer chitosan/montmorillonite nanocomposites: preparation and characterization. Polym Degrad Stabil. 2005;90:123-31.
13. Xu Y, Ren X, Milford A. Chitosan/clay nanonanocomposite film preparation and characterization. J Appl Polym Sci. 2006;99:1684-91.
14. Liu KH, Liu TY, Chen SY, Liu DM. Effect of clay content on electrostimulus deformation and volume recovery behavior of a clay–chitosan hybrid nanocomposite. Acta Biomater. 2007;3:919-26.
15. Liu KH, Liu TY, Chen SY, Liu DM. Drug release behavior of chitosan–montmorillonite nanonanocomposite hydrogels following electrostimulation. Acta Biomater. 2008;4:1038–45.

16. Yuan Q, Shah J, Hein S, Misra RDK. Controlled and extended drug release behavior of chitosan-based nanoparticle carrier. Acta Biomater. 2010;6:1140-8.
17. Depan D, Kumar AP, Singh RP. Cell proliferation and controlled drug release studies of nanohybrids based on chitosan-g-lactic acid and montmorillonite. Acta Biomater. 2009;5:93-100.
18. Salcedo I, Aguzzi C, Sandri G, Bonferoni MC, Mori M, Cerezo P, et al. In vitro biocompatibility and mucoadhesion of montmorillonite chitosan nanocomposite: A new drug delivery. Appl Clay Sci. 2012;55:131–7.
19. Salcedo I, Sandri G, Aguzzia C, Bonferoni C, Cerezoa P, Sánchez-Espejoc R, et al. Intestinal permeability of oxytetracycline from chitosan-montmorillonite nano-composites. Colloids Surf B. 2014;117:441-8.
20. Cojocariu A, Porfire L, Cheaburu C, Vasile C. Chitosan/montmorillonite composites as matrices for prolonged delivery of some novel nitric oxide donor Compounds based on theophylline and paracetamol. Cellulose Chem Technol. 2012;46(1-2):35-43.
21. Cojocariu A, Profire L, Aflori M, Vasile C. In vitro drug release from chitosan Cloisite 15A hydrogels. Appl Clay Sci. 2012;57:1-9.
22. Wei Fen Z, Xi Guang C, Pi Wu L, Qiang Zhi H, Hui Yun Z. Preparation and characterization of theophylline loaded chitosan/β-cyclodextrin microspheres. J. Mater. Sci. Mater. M. 2008;19:305-10.
23. Mastiholimath VS, Dandagi PM, Samata Jain S, Gadad AP, Kulkarni AR. Time and pH dependent colon specific, pulsatile delivery of theophylline for nocturnal asthma. Int J Pharm. 2007;328(1):49-56.
24. Berens AR, Hopfenberg HB. Diffusion and relaxation in glassy polymer powders. 2. Separation of diffusion and relaxation parameters. Polymer. 1978;19(5):489-96.
25. Yamashoji S, Asakawa A, Kawasaki S, Kawamoto S. Chemiluminescent assay for detection of viable microorganisms. Anal Biochem. 2004;333(2):303-8.
26. Cheaburu CN, Stoica B, Neamţu A, Vasile C. Biocompatibility testing of chitosan hydrogels. Rev Med Chir Soc Med Nat Iasi. 2011;115(3):864-70.
27. Noe DA, Weedn V, Beli WR. Direct spectrophotometry of serum hemoglobin: an allen correction compared with a three-wavelength polychromatic analysis. Clin Chem. 1984;30:627-30.
28. Dumitriu RP, Oprea AM, Cheaburu CN, Nistor MT, Novac O, Ghiciuc CM, et al. Biocompatible and biodegradable alginate/poly(n-isopropylacrylamide) hydrogels for sustained theophylline release. J Appl Polym Sci. 2014; 131(17):40733.
29. Chowdhury MA, Hill DJT, Whittaker AK. Vitamin B12 release from p(HEMA-co-THFMA) in water and SBF: A model drug release study. Aust J Chem. 2005; 58(6):451-6.
30. Oh JM, Cho CS, Choi HK. A mucoadhesive polymer prepared by template polymerization of acrylic acid in the presence of poly(vinyl alcohol) for mucosal drug delivery. J Appl Polym Sci. 2004;94(1):327-31.
31. Korsmeyer RW, Lustig SR, Peppas NA. Solute and penetrant diffusion in swellable polymers. I. Mathematical modeling. J Polym Sci Part B: Polym Phys. 1986; 24(2):395-408.
32. Ritger PL, Peppas NA. A simple equation for description of solute release II. Fickian and anomalous release from swellable devices. J Controlled Release. 1987; 5(1):37-42.
33. Ram FSF, Jardin JR, Atallah A, Castro AA, Mazzini R, Goldstein R, et al. Efficacy of theophylline in people with stable chronic obstructive pulmonary disease: A systematic review and meta-analysis. Respir Med. 2005;99(2):135-44.
34. Popa N, Novac O, Profire L, Lupusoru CE, Popa MI. Hydrogels based on chitosan–xanthan for controlled release of theophylline. J Mater Sci Mater Med. 2010; 21(4):1241-48.
35. Labacevski N, Zendeloska D, Sibinovska, O, Simeska S, Kikerkov I, Miloseviski P. Bull. Chem. Technol. Macedonia. 2003; 22:97.
36. Singh SK, Pandit JK, Mishra DN. Influence of drug solubility, drug polymer ratio, nature of coexcipients and thermal treatment on drug release from carbopol. Acta Pharma Sci. 2006;48:167–78.
37. De la Torre PM, Torrado S, Torrado S. Interpolymer complexes of poly(acrylic acid) and chitosan: influence of the ionic hydrogel-forming medium. Biomaterials. 2003;24(8):1459-68.
38. Korsmeyer RW, Gurny R, Doelker E, Buri P, Peppas NA. Mechanism of solute release from porous hydrophilic polymers. Int J Pharm. 1983;15(1):25-35.

39. Kubo W, Miyazaki S, Attwood D. Oral sustained delivery of paracetamol from in situ-gelling gellan and sodium alginate formulations. Int J Pharm. 2003;258:55-64.
40. Güneri T, Arici M, Ertan G. Preparation and diffusional evaluation of sustained-release suppositories containing ibuprofen microspheres. FABAD J Pharm Sci. 2004; 29:177-84.
41. Habibi Y, Lucia LA, editors. Polysaccharide building blocks: a sustainable approach to the development of renewable biomaterials. 1st ed. John Wiley & Sons; 2012.
42. Kim SK, editor. Chitin and chitosan derivatives: advances in drug discovery and developments. 1st ed. CRC Press; 2013.
43. Horn SJ, Eijsink VGH. A reliable reducing end assay for chito-oligosaccharides. Carbohydr Polym. 2004;56:35–9.
44. Domszy JG, Roberts GAF. Evaluation of infrared spectroscopic techniques for analyzing chitosan. Makromol Chem. 1985;186:1671-77.
45. Mucha M, Pawlak A. Complex study on chitosan degradability. Polimery. 2002;47:509-16.
46. ISO 10993-5:1999. Biological evaluation of medical devices. Part 5: Tests for *In vitro* cytotoxicity.
47. ASTM standard practice F 756-00. Assessment of hemolytic properties of materials.
48. Vassileva V, Grant J, De Souza R, Allen C, Piquette-Miller M. Novel biocompatible intraperitoneal drug delivery system increases tolerability and therapeutic efficacy of paclitaxel in a human ovarian cancer xenograft model. Cancer Chemother Pharmacol. 2007;60(6):907-14.
49. OECD Guidelines for the Testing of Chemicals, Acute Oral Toxicity—Up-and-Down-Procedure (UDP); 2008.
50. Schneck K, Washington M, Holder D, Lodge K, Motzel S. Hematologic and serum biochemical reference values in nontransgenic FVB mice. Comp Med. 2000;50(1):32-5.
51. Wanjun T, Cunxin W, Donghua C. Kinetic studies on the pyrolysis of chitin and chitosan. Polym Degrad Stab. 2005; 87(3):389-94.
52. Arora S, Lal S, Kumar S, Kumar M, Kumar M. Comparative degradation kinetic studies of three biopolymers: Chitin, chitosan and cellulose. Appl Sci Res. 2011;3(3):188-201.
53. Georgieva V, Zvezdova D, Vlaev L. Non-isothermal kinetics of thermal degradation of chitosan. Chem Central J. 2012;6:81.
54. Vasile C, Darie RN, Cheaburu-Yilmaz CN, Pricope GM, Bracic M, Pamfil D, et al. Low density polyethylene–Chitosan composites. Composites: Part B. 2013; 55:314-23.
55. Wesolowski M, Szynkaruk P. Thermal decomposition of methylxanthines interpretation of the results by PCA. J Therm Anal Calorim. 2008;93(3):739-46.
56. Wesoowski M, Szynkaruk P. Thermal decomposition of purine derivatives used in medicine. J Therm Anal Calorim. 2001; 65:599-605.
57. European Pharmacopoeia, 3rd ed., Council of Europe, Strasbourg Cedex; 1997.
58. Poon L, Wilson LD, Headley JV. Chitosan-glutaraldehyde copolymers and their sorption properties. Carbohydr Polym. 2014;109:92-101.
59. Ritger PL, Peppas NA. A simple equation for desciption of solute release I. Fickian and non-Fickian release from non-swellable devices in the form of slabs, spheres, cylinders or discs. J Controlled Release. 1987;5(1):23-36.
60. Hua S, Yang H, Wang A. A pH-sensitive nanocomposite microsphere based on chitosan and montmorillonite with in vitro reduction of the burst release effect. Drug Dev Ind Pharm. 2010;36:1106-14.

APPENDIX

Supplementary information regarding details of the spectroscopic and thermal behavior results are added within this section.

Table 1. The FT-IR bands assignment for the systems based chitosan

Band (cm^{-1})	Sample			Assignment
	CS	CS-Na^{+}MMT 5%	CS-NaMMT 5% -GA	
650	652	653	622	Amide group
900	897	-	861 ; 936	Carboxyl, Furan cycle
1000	1027 1065	1024	1030	Carboxyl, ether groups
1100	1152	1152	-	Aliphatic primary and secondary amine groups
1200	1257	1256	1262	Amine and lactone groups
1300	1380	-	1375	Carbonyl, tertiaryamine group
1400	1408	1407	-	Carboxyl, amine
1500	1549	1545	1562	Amine groups
1600	1635	1635	1651	Amine groups I
1700	-	-	1708	Carbonyl groups
1800	-	-	1897	Carbonyl, lactone
1900	-	1987	1984	Ammonium groups
2000	2052	2052	2050	Amine groups and ammonium salts
2100	2168	2167	2144 2167	Amine groups and silicates
2200	-	-	2292	Amine groups and silicates
2300	2322	2323	2322	Amine groups and salts
2800	2882	2882	2870	Carboxyl, amine cetone groups
2900	2924	2926	2937	Carboxyl and intramolecular hydrogen-bonded hydroxyl groups
3200	3286	3260	-	Intramolecular OH groups intramolecular hydrogen-bonded hydroxyl groups
3300	3348	3348	3357	Intramolecular hydrogen-bonded hydroxyl groups, carboxyl and amine II groups

Table 2. NIR bands assignment for the systems based chitosan

Theophylline	CS/GA		CS/Na^+MMT/GA		Assignment
	Without THP	With THP	Without THP	With THP	
1170	1158	1166	1154	1158	C-H second overtone
1367	1363	1371	1354	1363	1 st C-H overtone and combinations
		1438*		1437*	N-H stretch 1st overtone
		1514*		1530*	N-H stretch 1st overtone
1676	1630	1630*	1635*	1670	C-H stretch 1st overtone
	1670	1664	1672		
1710	1710	1718	1731*	1718*	C-H stretch 1st overtone
1819*	1814*	1831*	1869	1824*	C-O and O-H combinations
1882	1863	1873		1864	
	1999				O-H bend second overtone
2004	2074	2003	2015	2015	O-H and N-H combinations
		2095		2095*	
2137	2141	2141*	2145*	2137*	N-H combinations
		2195*	2199*	2199*	
2254	2254	2258	2245	2258	O-H and C-H combinations
		2291			
2321	2324	2325	2321	2325	C- H stretch/CH_2 deformation
2379	2375	2375	2379*	2375*	
2429	2429	2434	2429	2425	C- H and C-C combinations
2475		2475		2475	C-N- C stretch overtone

Table 3. Temperature ranges determined from TG and DTG curves

Sample	Step II			Step III			Step IV			ΔW (%)			
	Ti	Tm	Tf	Ti	Tm	Tf	Ti	Tm	Tf	I	II	III	IV
CS	153	276	436							13	56		
CS/GA	102	212; 257	337	355	440	557				4	48	28	
CS/GA/T	178	273	352	490	572	620				9	50	37	
CS/Na^+MMT/GA	150	185sh; 283	390			505				0.5	31	65	
CS/Na^+MMT/GA/T	162	247 ; 271sh	330	406	434	479	498	575	622	8	31	25	35

Ti – onset temperature; Tm – peak temperature; Tf – end temperature

Peer-review history:
The peer review history for this paper can be accessed here:
http://www.sciencedomain.org/review-history.php?iid=985&id=14&aid=8396